# Review of Environmentally Assisted Cracking

K. SADANANDA and A.K. VASUDEVAN

Many efforts have been made in the past by several researchers to arrive at some unifying principles governing the embrittlement phenomena. An inescapable conclusion reached by all these efforts was that the behavior is very complex. Hence, recognizing the complexity of material/environment behavior, we focus our attention here only in extracting some similarities in the experimental trends to arrive at some generic principles of behavior. Crack nucleation and growth are examined under static load in the presence of internal and external environments. Stress concentration, either pre-existing or *in-situ* generated, appears to be a requirement for embrittlement. A chemical stress concentration factor is defined for a given material/environment system as the ratio of failure stress with and without the damaging chemical environment. All factors that affect the buildup of the required stress concentration, such as planarity of slip, stacking fault energy, *etc.*, also affect the stress-corrosion behavior. The chemical stress concentration factor is coupled with the mechanical stress concentration factor. In addition, generic features for all systems appear to be (a) an existence of a threshold stress as a function of concentration of the damaging environment and flow properties of the material, and (b) an existence of a limiting threshold as a function of concentration, indicative of a damage saturation for that environment. Kinetics of crack growth also depends on concentration and the mode of crack growth. In general, environment appears to enhance crack tip ductility on one side by the reduction of energy for dislocation nucleation and glide, and to reduce cohesive energy for cleavage, on the other. These two opposing factors are coupled to provide environmentally induced crack nucleation and growth. The relative ratio of these two opposing factors depends on concentration and flow properties, thereby affecting limiting thresholds. The limiting concentration or saturation depends on the relative chemistry of environment and material. A dynamic dislocation model is suggested to account for crack growth.

## I. INTRODUCTION

THE purpose of our analysis is to extract some generic principles governing the embrittlement phenomena that encompass a wide variety of materials, material microstructures, and environments. The materials include brittle materials such as glasses and ceramics, more ductile metals, alloys, single crystals, and complex engineering materials with relatively high toughness in an inert environment. Environments include external gaseous, aqueous, liquid metal environments as well as internal hydrogen or internal embrittling elements such as Pb and Cd. There is an extensive literature on each of these materials and environments, and many review articles exist summarizing, classifying, or unifying the principles underlying the embrittlement phenomenon.[1–20] Gangloff[11] provided an exhaustive list of literature references in his review on hydrogen embrittlement. In the present article, we only highlight general behavior and cover only those references and analyses that are pertinent to the generic principles involved in embrittlement phenomenon. Our analysis pertains specifically to stress corrosion and not to general corrosion, exfoliation, or time-dependent creep.

## II. GENERAL BEHAVIOR

### A. *Crack Nucleation*

Three distinct types of specimens have been used to experimentally characterize and quantify the embrittlement process: (1) smooth specimens under uniaxial loading; (2) fracture mechanics specimens with initially sharp fatigue precracks; and (3) notch tensile specimens with finite depth, which can be considered as an intermediate between the first two. In the limit of infinite notch-tip radius, they behave like smooth tensile specimens, and in the limit of zero radius, they behave like cracked specimens. We may note here that atomically sharp crack cannot be sustained in a material due to singularity in stresses at the crack tip. Hence, a realistic case involves crack tip core relaxations in brittle materials such as glasses[21] or localized crack tip plasticity resulting in a finite radius in ductile materials. The assumption of some minimum critical crack tip radius is not far from reality,[22,23] to characterize the behavior.

Figure 1 highlights the behavior of smooth, notch, and cracked specimens. Under sustained load or stress

K. SADANANDA, Consultant, is with Technical Data Analysis, Falls Church, VA 22042. Contact e-mail: kuntimaddisada@yahoo.com A.K. VASUDEVAN, Scientific Officer, is with the Office of Naval Research, Arlington, VA 22203.

in an aggressive environment, a smooth specimen fails in time. Experimental results indicate that the stress to fail reaches an asymptotic limit, indicated by a threshold stress, $\sigma_{th}$. In the case of a fracture mechanics specimen, the asymptotic limit corresponds to a threshold stress intensity factor, $K_{th}$. There are predominately two factors that govern these thresholds: one is the chemical concentration and the other is material flow properties, such as yield stress, slip mode, work hardening, *etc.*

Figures 2(a) and (b) give some examples[24,25] showing that the thresholds reach asymptotic levels as a function of (a) concentration of the chemical agent, for a given yield strength; and (b) yield stress for a given concentration. There is a limiting threshold as a function of concentration showing the saturation effect of the environment, indicative of some maximum occupancy sites available for the reactive species. The limiting threshold also indicates that some minimum stress is required at any concentration, to create fresh new surfaces. That means chemical force alone is not sufficient to create the cracked surfaces. On the other hand, as the concentration approaches zero, the limiting value converges to fracture toughness value, $K_{IC}$, of the material in an inert environment. This indicates that stress alone can provide the conditions necessary to create fresh new fracture surfaces. This difference between the chemical stress and the mechanical stress has to be noted. Hence, one can look at the embrittlement phenomenon as a reduction in the stress necessary for nucleation/propagation of a crack or the energy necessary to create two new fracture surfaces. This reduction in the applied stress due to embrittlement in relation to the stress in inert environment becomes a measure of the chemical driving force expressed in terms of mechanical equivalent stress. Essentially, it is the chemical potential gradient providing the additional driving force that is needed for nucleation/propagation of a crack in a material, in creating new surfaces. Thus, there are predominantly two factors that govern the SCC behavior: the chemistry of the environment and the material flow properties. Just as we define the stress concentration factor as the ratio of nominal stress with and without a notch, we can loosely define the equivalent "chemical stress concentration factor" for a given material/environment system as the ratio of failure stress with and without the chemical environment. Effectiveness of a particular environment or chemical stress sensitivity in reducing the strength of a given material can thus be quantified. The chemical stress concentration factor depends on all the variables that affect the crack tip chemical environment in reducing the failure stress of the material in that environment. The requirement of a minimum threshold stress at any concentration also undermines the chemical dissolution process as the governing mechanism of crack growth, unless dissolution is shown to require some minimum stress. Some important considerations are now presented to
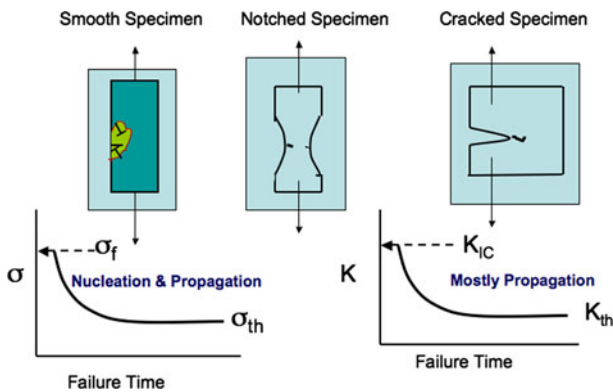


Fig. 1—Comparing sustained load stress-corrosion behavior in smooth and cracked specimen. Time to failure depends on remote stress with existence of thresholds below which no failure occurs. Stress concentration is required for embrittlement. Localized plasticity generates stress concentration in a smooth specimen. Notch specimen behavior is in between the smooth and cracked specimens.
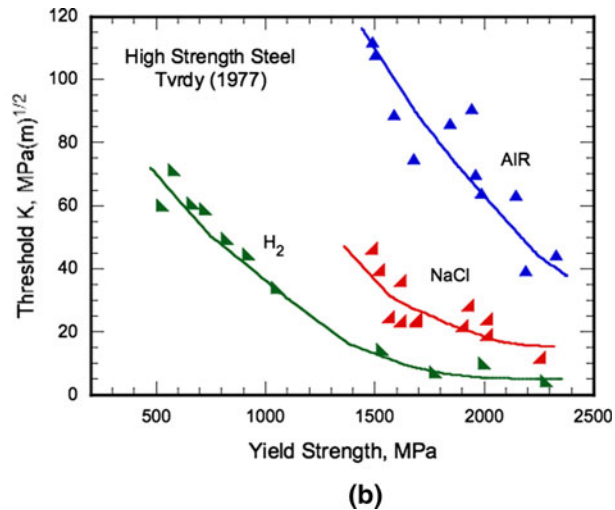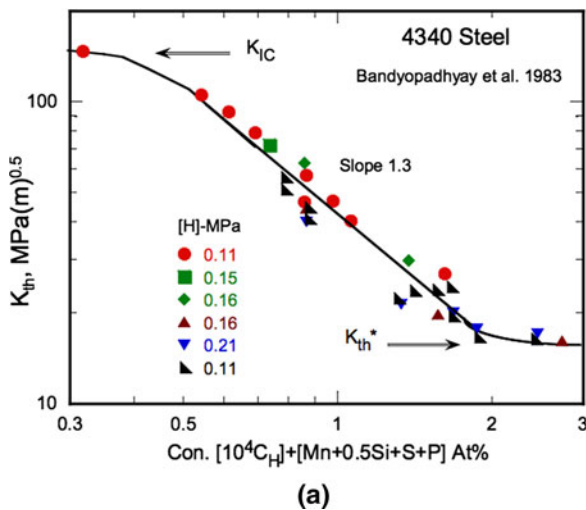


Fig. 2—(a) Example showing threshold, $K_{th}$, approaches a limiting value as a function of concentration, indicating that the chemical effects gets saturated. (b) Examples showing the threshold $K_{th}$ levels of a limiting value as a function of yield stress.

understand the role of the chemical environment by examining the liquid metal embrittlement (LME) results.

Extensive experiments[2] on LME have revealed the following.

(1) Stress-strain behavior is not notably affected by the environment; mostly fracture strain is drastically reduced.[26–28] That is, the stress-strain curves are almost identical other than the reduction in the fracture strain in the presence of a liquid metal. In essence, the yield stress and strain hardening are unaffected by the environment other than the stress (strain) necessary for crack initiation and growth. The reduced fracture strain is a reflection of the reduction in cohesive forces for crack formation and growth.
(2) Experimental results[29] on Ni single crystals showed that LME occurs only in notched specimens but not in smooth specimens.
(3) Similar results were obtained in fine-grained Ni-polycrystals. Hence, the pre-existing stress concentration appears to be necessary for single crystals as well as the fine-grain specimens.
(4) On the other hand, LME occurred in coarse-grained Ni-polycrystals even in un-notched specimens.

The following conclusions can be reached based on the preceding observations. A stress concentration is essential for embrittlement to occur. This required stress concentration can be pre-existing, as in a notched or cracked specimen, or it has to be generated by an *in-situ* deformation process, as in a smooth specimen. Heterogeneity of slip in coarse-grained specimens provides the conditions for the *in-situ* buildup of stress concentrations, in favorably oriented grains. Thus, localization of slip becomes an important factor in building the stress concentrations for nucleation of a crack. This is schematically indicated in the smooth specimen in Figure 1. Hence, factors that enhance localization of slip enhance the susceptibility for stress corrosion. These include the planarity of slip or reduction in stacking fault energy, ordered precipitates, coarse grain size, *etc*. Similarly, existence of multiple slip systems that help in homogenization of slip, such as in fcc materials, fine-grain size, *etc*., enhance the resistance to stress corrosion. Hence, stress concentration seems to be an important factor, while all others seem to be subsidiary factors that help in creating the needed stress concentration.

To facilitate crack nucleation, the stress concentration by slip has to occur. This can be accomplished by dislocations piled up against grain boundaries or insurmountable barriers or by the coarse slip-band formation at a free surface. Two questions are pertinent here in relation to LME in a smooth tensile sample. First, for embrittlement to occur, how the liquid metal at the surface can "act" at the internal stress concentration formed due to dislocations piled up at a distance, *d*, from the surface, where *d* is the grain size. Second, the concentrated stresses are more likely to nucleate a crack in the second grain further away from the surface or at

least along an orientation perpendicular to the pile-up plane as the dislocations coalesce to form a crack as in the Stroh[30] or Smith and Barnby[31] model. To overcome such problems, Gilman[32] proposed a crack formation along the original slip plane, where the dislocations in the piled-up configuration are absorbed by the crack to make it energetically feasible, as there is no concentration of the tensile stress on that plane. A similar mechanism was proposed by Mura[33] in accounting for crack nucleation along the persistent slip bands in fatigue. In all these cases, the cracking occurs along the slip plane rather than on a cleavage plane. To address the first question, transport of liquid atoms from the surface to the interior *via* dislocations or by diffusion becomes a necessary condition for embrittlement, if the stress concentration is not surface connected. Transport of smaller atoms such as hydrogen by dislocations has been suggested,[34] but not of liquid metal atoms such as Hg. The other alternative transport process is by diffusion, a preferred path being a grain boundary in a polycrystal. In any case, the transport process makes crack nucleation a time-and stress-dependent phenomenon. Incubation-time experiments along with the activation-energy measurements would help to resolve this issue.

Figures 3(a) and (b) show the stress *vs* time to failure data for Al alloys in different environments.[35–39] Figure 3(a) shows that the embrittlement in Hg is very rapid at room temperature in 2024 alloy, while it is delayed at higher temperature, probably due to increased tendency to form an amalgam with the base metal. Figure 3(b), on the other hand, shows a much delayed failure in 5083 alloy in Hg, but this delay could be due to the presence of an oxide scale.[40] Elegant work by Chu *et al.*[41] shown in Figure 4 demonstrates the nature of the cracking process that could be involved, even in LME. Compact tension specimens of Al 7075 alloy specimens with a 30 deg notch root radius were loaded under tension and compression in the Ga-LME environment. The incubation times for crack nucleation were measured at various constant stress levels. The important points to note here are (a) the incubation times are shorter under tension compared to those under compression, and (b) crack nucleation occurred at the notch tip for tensile specimen, while it occurred far ahead of the notch, when subjected to compression. The insert figure shows the nucleation of a crack ahead of the notch tip in compression. Diffusion of Ga into the region of tensile stresses was involved, assuming that all the precautions were taken to seal the Ga activity from the sides of the sample.

Figure 5(a) shows the role of Cd in embrittling steel at different temperatures[42] ranging from 503 K to 633 K (230 °C to 360 °C). The melting point of Cd is 594 K (321 °C). Embrittlement occurs in the presence of both solid and liquid Cd. Note that the curves essentially run parallel, and for a given stress, the failure time decreases with increasing temperature. It is assumed that there is sufficient vapor pressure of Cd to contribute to embrittlement even in solid state. In the liquid state, the embrittlement is very rapid with failure occurring in minutes. The Arrhenius plot (Figure 5(b)) in terms of
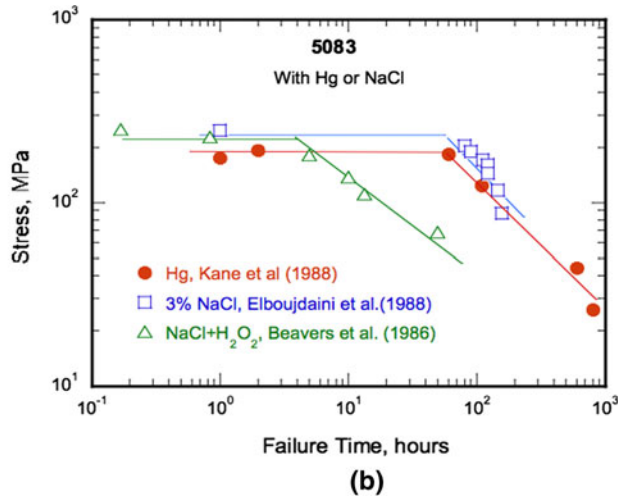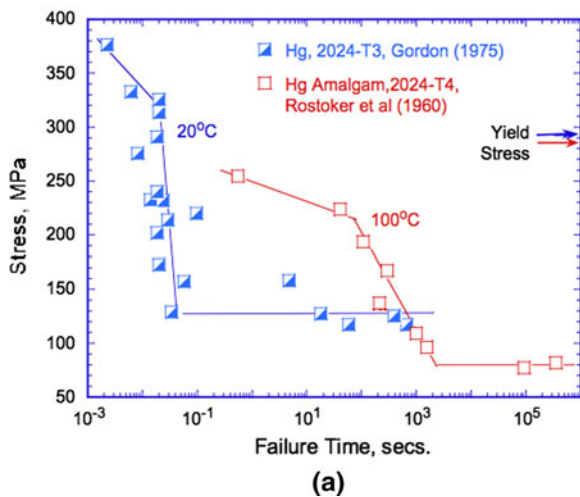
Fig. 3—(a) Stress *vs* failure time in Al alloy in Hg. Steep L shape with fractions of seconds shows the rapid rate of crack nucleation and growth. At high temperature, failure times are large either due to amalgamation or oxide formation. (b) Stress *vs* failure time of another Al alloy in different environments where failure times are reasonably large at low stresses.
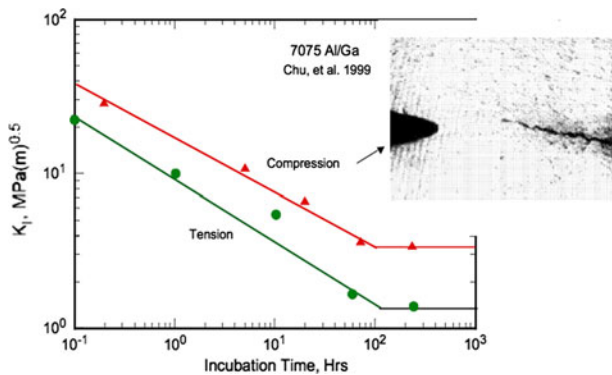


Fig. 4—Incubation times for crack nucleation in Al alloy with Ga under tension and compression. During compression, crack nucleation occurs way ahead of the notch, where tensile stresses may be present. Diffusion of the Ga is envisioned.

rate (1/time) *vs* 1/*T* shows that the apparent activation energy is about 168 kJ/mole, with the liquid Cd data falling on the same line as that of solid Cd, indicating that the embrittling process remains the same. Similar results were obtained in 4140 steel with indium by Gardon and An[43] and by Druschitz[44] with In and In-Sn, as shown in Figure 5(c). In all these cases, the activation energy is quite high, characteristic of sold-state diffusion. Lynch[45] has compared diffusion coefficients extracted from LME data (or, to be more specific, solid metal induced embrittlement (SMIE)) with the surface self-diffusion kinetics and showed that the diffusion coefficients in SMIE are two orders of magnitude lower. He suggests that the lower values are due to the assumed diffusion distances used in the calculations, which are larger than the actual values. In any case, the conclusion is that the diffusion kinetics govern the kinetics of embrittlement. On the other hand, Kamdar[46] provides an example of the brass-Hg system (Figure 6), which shows that activation energy is very low under LME and corresponds more to liquid flow to the crack

tip than any diffusion ahead of the crack tip. In fact, at higher temperatures, the process becomes complex, indicating a change in the mechanisms. Wei and Gao[47] classify material behavior in aqueous environments using a (*da/dt*)-1/*T* plot and attribute changes in the activation energies to changes in mechanisms, as indicated in Figure 7. In general, incubation times have been observed[48] in many corrosion-susceptible alloys, as shown in Figure 8(a). With a decrease in initial stress intensity, the incubation time increases, and the slope on a log-log plot is close to 0.5, characteristic of diffusion-related phenomenon. Slopes less than 0.5 have also been observed, and Figure 8(b) shows such an example. Here, the actual reaction kinetics at the crack tip can govern the embrittlement process, which includes incubation time for crack nucleation. At this stage, we do not know what specific crack tip environmental reaction kinetics can be related to a particular slope of incubation time *vs* K plot.

Some authors[49–52] have attributed LME to the crack tip dissolution process, wherein the intermittent crack tip plasticity facilitates crack opening for liquid flow in the presence of capillary and the viscous forces and intermittent ledges formed cut down the distances for transport for precipitating the dissolved metal atoms. Dissolution, diffusional transport, and re-precipitation are involved in contributing to the liquid embrittlement. We may note here that, although Figures 5(b) and (c) indicate that there is no change in the activation energies from liquid to solid metal embrittlement, discrete jumps in kinetics have been noted[43] in going from the solid to liquid state of the embrittling element.

Dissolution of grain boundary precipitates was also suggested as a viable stress corrosion mechanism in some systems, particularly when reactive elements such as Li, *etc.*, are present. Kamdar[2] has listed several objections to this type of mechanism in LME. There are also many examples wherein increasing the grain boundary precipitation causes reduction in crack growth rate rather than the increase to be expected from

Fig. 6—Low activation energy for embrittlement in brass/Hg system.





Fig. 7—Change in the activation energies or mechanism of crack growth with concentration and temperature in 4340 steel with hydrogen.
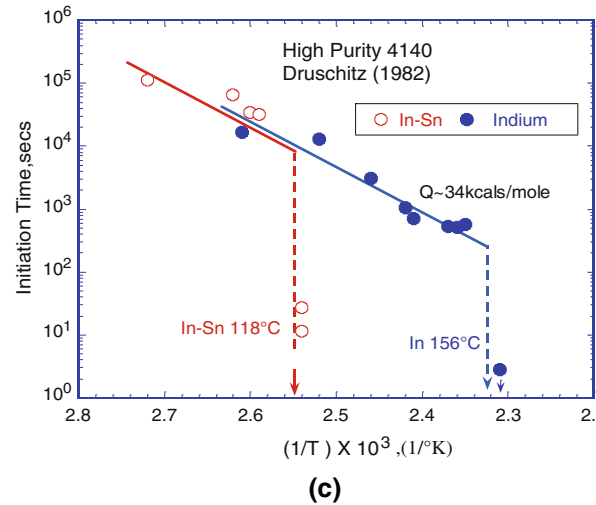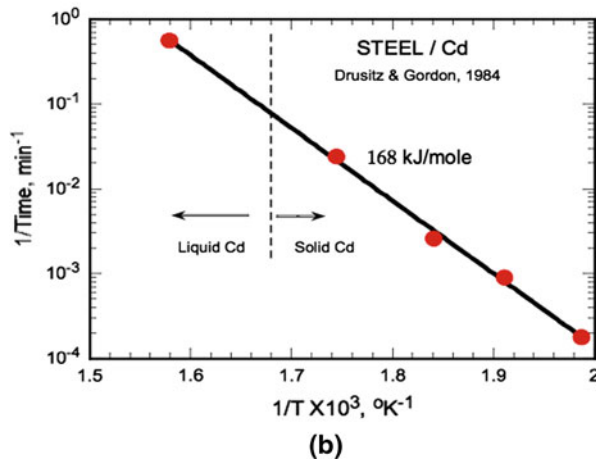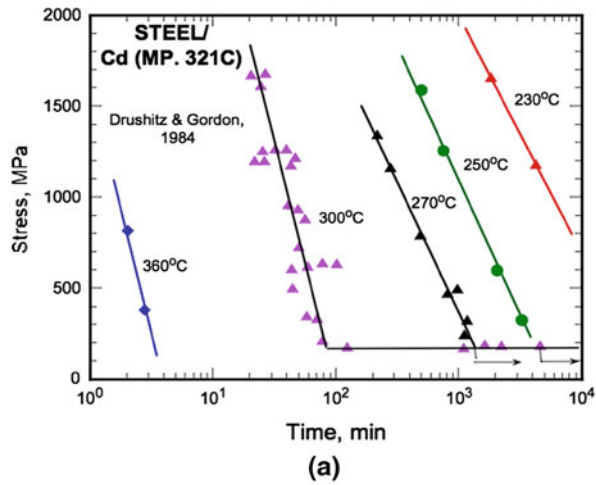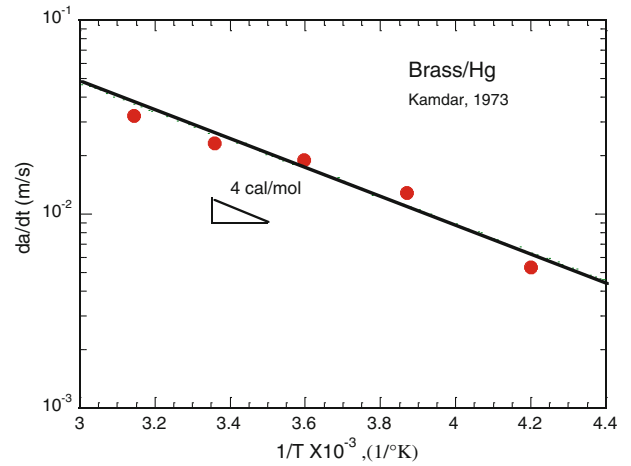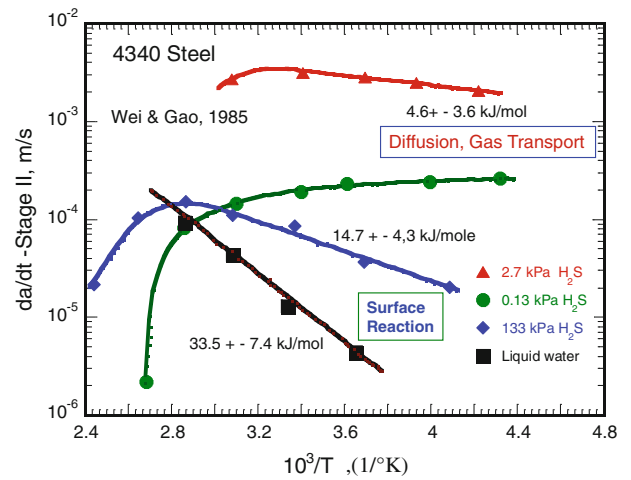
Fig. 5—(a) Cadmium embrittlement of a steel below and above the melting point of Cd. (b) Activation energy for Cd embrittlement of steel showing the data above and below the melting point of Cd fall on the same line. (c) Plot of initiation time vs inverse of temperature for 4140 steel with In and In-Sn.

dissolution kinetics. On the other hand, there is evidence that shows preferential dissolution of the precipitates in reactive environments contributing to SCC. A more detailed analysis of precipitation or aging effects is discussed elsewhere.[53] The presence of sharp

crystallographic features observed on many fracture surfaces weighs against the dissolution type of mechanisms.[40] Nevertheless, a detailed study of mating fracture surfaces under LME and stress corrosion, which is currently lacking, can help resolve these issues. Similarly, several investigators[54–56] have shown that electrochemical factors at the crack tip are important. While these may be important for aqueous solutions, we are looking at the general behavior that is common to both aqueous and nonaqueous environments. Another process suggested is the time-dependent plastic flow (creep rates) as a means of generating the fresh crack tip surfaces for chemical reactions to proceed, and this may be pertinent at slightly higher temperatures where creep rates can be significant for materials of concern.[57,58]

In summary, nucleation or growth of cracks requires (a) a threshold stress or stress intensity that varies with yield stress or plastic flow properties or factors that affect them; (b) a critical maximum chemical concentration suggestive of a saturation effect; and (c) a localized plasticity that is either required to establish in-situ stress
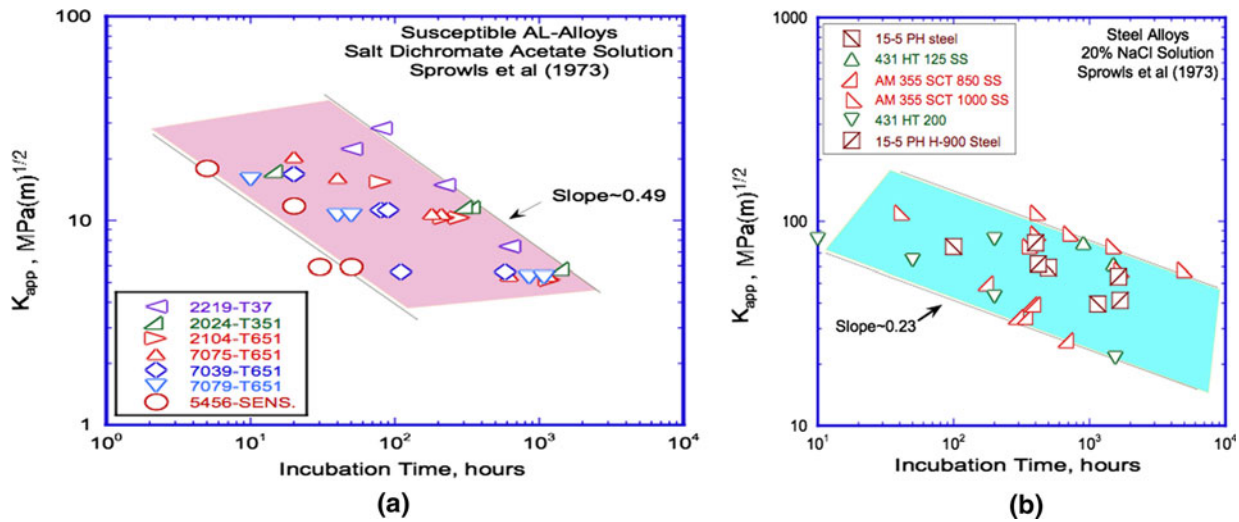
Fig. 8—(a) Applied stress intensity *vs* incubation time for Al alloys susceptible to corrosion. (b) Applied stress intensity *vs* incubation time for steels that are less susceptible to corrosion.

concentrations as in smooth specimens, or required to provide a short transport distance for chemical species to ingress, or an unavoidable process that accompanies the crack growth. There are also conditions under which the plasticity itself provides a requirement for embrittlement, as in hydrogen enhanced local plasticity (HELP) mechanisms, which will be discussed later. In all cases, the incubation times are significant except in cases where the reaction kinetics at the crack tip itself governs the crack growth kinetics, a clear example being the effect of humidity in the embrittlement of glasses.[16] Even in these cases, the reduction of rate of transportation of embrittling species toward the crack tip, or by their dilution with inert constituents, increases the threshold stress necessary for nucleation and growth of cracks.[59,60] The effect of notch tip radius on incubation in some material/environment systems also supports the diffusion mechanisms governing the nucleation and growth kinetics.[61–63] The question whether the governing embrittling mechanisms take place at the crack tip or ahead of the crack tip gets camouflaged if the peak hydrostatic stress, where crack nucleates, is close to the crack tip. It was shown[61] earlier using notches of varying severity that microcrack formation occurs ahead of the notch tip, but within its plastic zone. These results also affirm that diffusion distances are limited very close to the crack or notch tip.

We will next examine the crack growth process along with the associated fractographic information that is available in the literature to understand the crack growth kinetics. The question that could arise is whether crack nucleation kinetics differ from the crack growth kinetics, as in, for example, fatigue, with the recognition that it is always difficult to separate or distinguish when the nucleation ends and the propagation begins.

### B. Crack Growth Behavior and Fractographic Analysis

Figures 9(a) and (b) show the variation of threshold stress intensity, $K_{th}$, with hydrogen concentration from different environmental sources and sample thicknesses in Ni-base superalloys, identifying the dominant mechanism for crack growth in each H-concentration regime. Some inferences can be made. First, there is a change in slope in $K_{th}$ *vs* hydrogen concentration, and the slope changes seem to correlate with the change in the dominant fracture mechanism. Understandably, plane stress seems to favor microvoid formation and coalescence, while plane strain favors the crystallographic faceted or cleavage mode of growth. Since alloy 718 is a Ni-base superalloy, the faceted growth occurs on {111} planes, which are slip planes rather than cleavage planes. Similar cleavage on slip planes was reported in pure Ni under hydrogen[64] atmosphere. Such faceted growth on slip planes is not uncommon and has been observed during fatigue crack growth.[65] In addition, at low concentrations of hydrogen, microvoid coalescence occurs, while at higher concentrations, either faceted crack growth (Figure 9(a))[66,67] or intergranular crack growth (Figure 9(b)) is favored.[68–70]

The resulting crack growth rates as a function of the stress intensity factor $K$ are represented schematically in Figure 10(a). Type I is characterized by well-defined threshold, stages I through III, where stage II corresponds to a plateau region with crack growth rates, $da/dt$, remaining constant in some range of $K$. Type II is characterized by lack of the well-defined plateau region where the growth rates increase with increasing $K$. However, there is a definite change in the slope of the $da/dt$ *vs* $K$ curve in some materials in going from stage I to stage II. The curves are similar to those normally observed in fatigue, with increasing $K$ results in increasing crack growth rate. The stage III crack growth is characteristic of the overload fracture process common to all subcritical crack growth. Endo *et al.*[71] show, in Figure 10(b), that this change in the type can occur as a function of thickness for the material/environment/test conditions. With increasing thickness, a shift from type I to type III occurs, thus plane stress favoring a well-defined plateau stage.
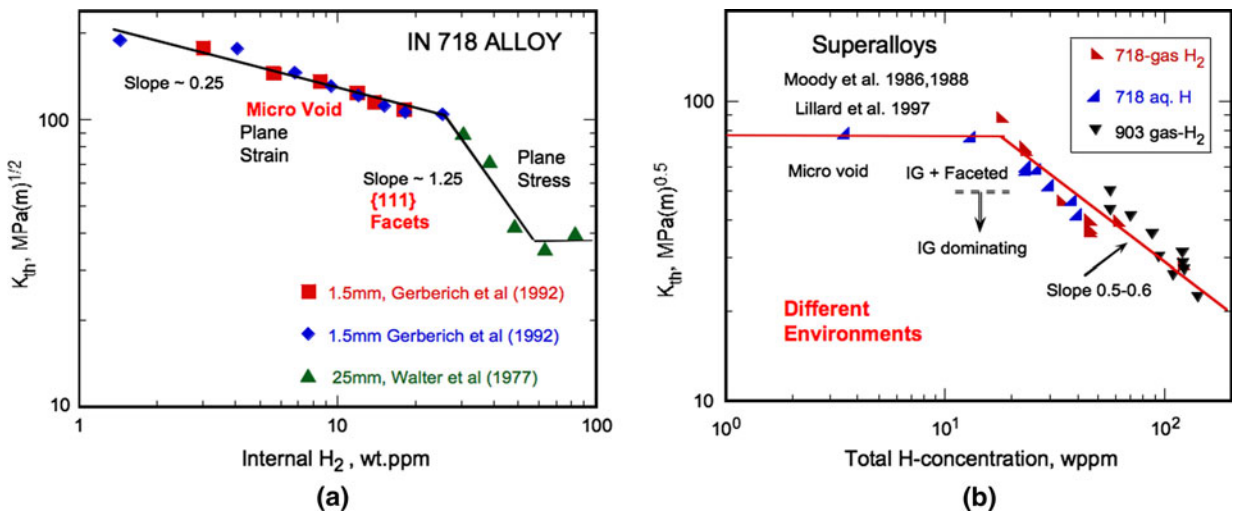
Fig. 9—(*a*) Threshold stress intensity *vs* internal hydrogen concentration for a superalloy 718. (*b*) Threshold *vs* H concentration for superalloys in gaseous and aqueous solutions, independent of the nature of source for H is evident.
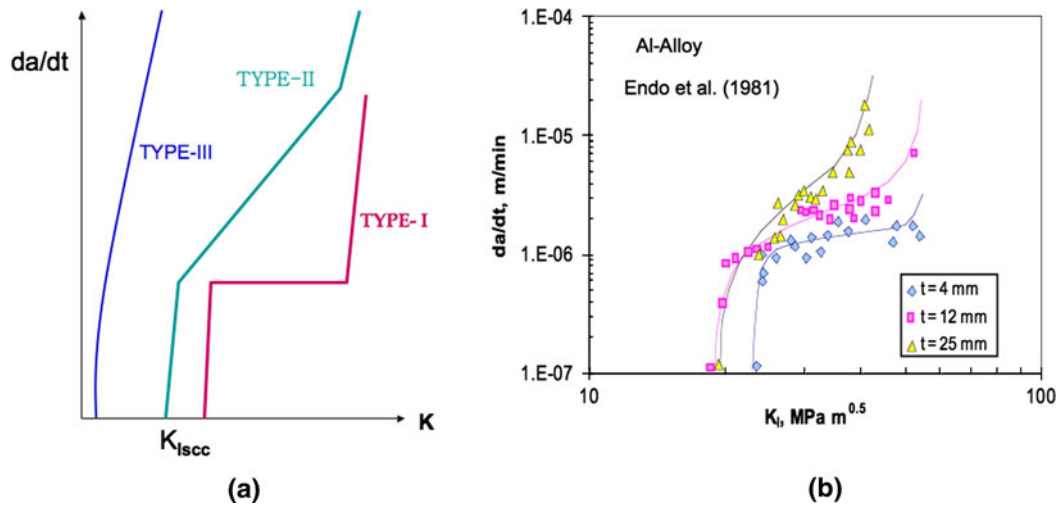


Fig. 10—(*a*) Classification of *da/dt vs K* curves into three types. (*b*) The type of *da/dt–K* curve changes with increase in thickness of the specimen.

Figure 11 shows an example where all three types of behavior can be noted with the change in H concentration[72] in IN-718 alloy. For concentrations less than 7 wt ppm, there is no well-defined plateau region, although there is a small change in the (*da/dt*) *vs K* curve when the concentration is 3 wt ppm. A well-defined plateau exists for concentrations 7 to 14 wt ppm. At still higher concentrations, the behavior is similar to type I but occurs at a much lower threshold *K*. Figure 12 shows the corresponding fractography. Three distinct modes of crack growth can be identified. At high concentrations, fracture is a faceted cleavage mode on {111} slip planes. At concentrations less than 16 wt ppm, distinct stage II was observed with crack growth occurring by void nucleation and coalescence. Here, large carbides form nuclei for voids. Further lowering the concentrations, there is no observable stage II, and the crack growth exhibits microvoid coalescence,

but on a finer scale. Here, void nucleation may still be occurring at smaller carbide sites or at some other heterogeneities.

These results indicate that the steady-state stage II, where the crack growth rate is independent of the remote applied *K*, is concentration dependent. Plateau is absent at high and low concentrations. The *δK* range (width of the plateau) where plateau occurs is shown for IN-625 alloy in Figure 13. This *δK* range could be dependent on both material and environmental chemistry. In addition, it could also depend on test method, *viz.* constant displacement, constant loading rate, or constant load tests. Lack of observation of plateau, therefore, is not an invalidation of the test method; it only means that the tests or material conditions are not suitable to establish the steady-state conditions in which crack growth is purely reaction/transport limited. In the range where there is a steady state, the plateau velocity

increases with concentration (Figure 14). Hence, at any given concentration (within the range that plateau is observable), steady-state conditions are established by limiting conditions, either by transport or crack tip reaction. Concentration dependence of plateau velocity has been observed in many systems.[73–75] Gangloff[11] showed that the stage II crack growth rates varied directly with hydrogen diffusivity (Figure 15) for various materials.

The question arises whether the lack of observation of a plateau at low and high concentrations in Figure 14 is due to a change in mechanism of crack growth or the test conditions, or whether some constraints imposed in the tests were not sensitive for stage II observation. The diffusivity of hydrogen in a metal is a function of the initial concentration.[11] Hence, for any given concentration, steady-state kinetics are established ahead of a moving crack tip. However, with decreasing concentration of hydrogen, the role of secondary traps becomes increasingly dominant. In steels as well as in superalloys, carbides form secondary traps for hydrogen. With decreasing hydrogen concentration, the mechanism of cracking changes to void formation at carbides that act as hydrogen traps. Presumably these carbides are within the plastic zone of the crack tip stress field, where tensile stresses are sufficiently high to cause void formation, growth, and coalescence. The mechanisms are similar to those envisioned by Rice and Johnson.[77] Cleavage fracture by the ductile process in steels was analyzed by Ritchie et al.[78]
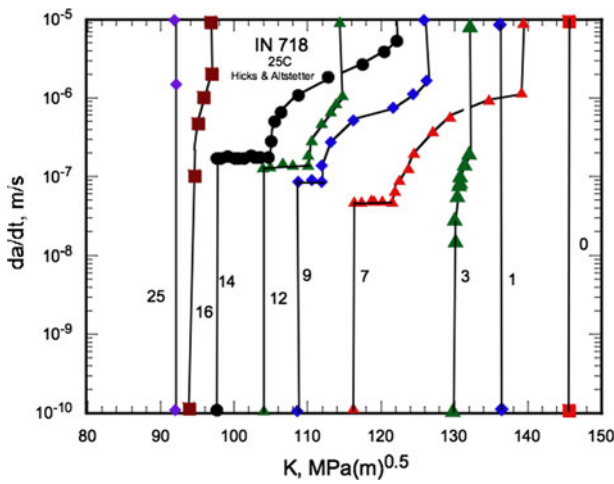


Fig. 11—Change in the da/dt vs K behavior with change in H concentration. Plateau was observed in some range of H concentration.
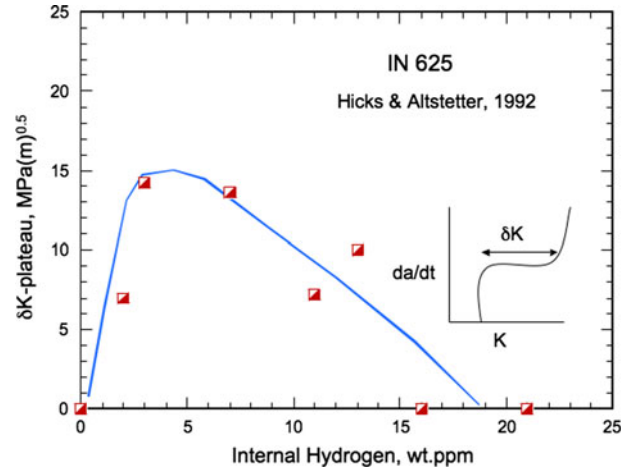


Fig. 13—K range at plateau velocity as a function of H concentration. Maximum plateau range was observed at some intermediate concentration with its absence at low and high concentrations.
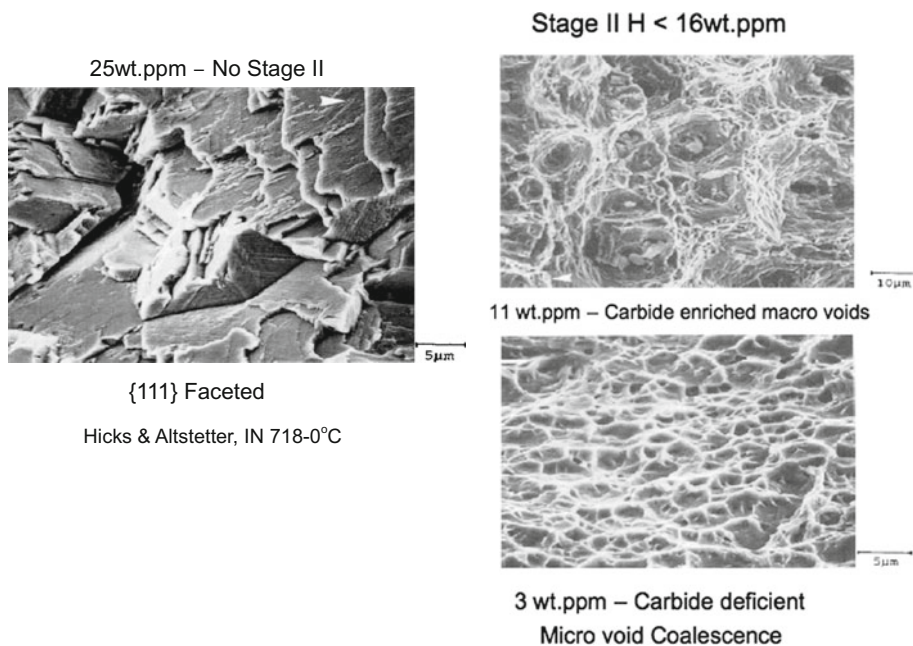


Fig. 12—Fracture appearance changes from faceted to carbide-enriched macrovoid to microvoid coalescence with H concentration.
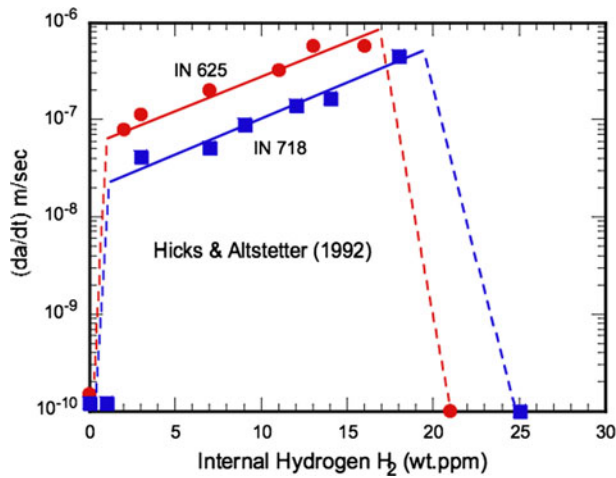
Fig. 14—Plateau velocity increases with concentration in the range where it is observed.
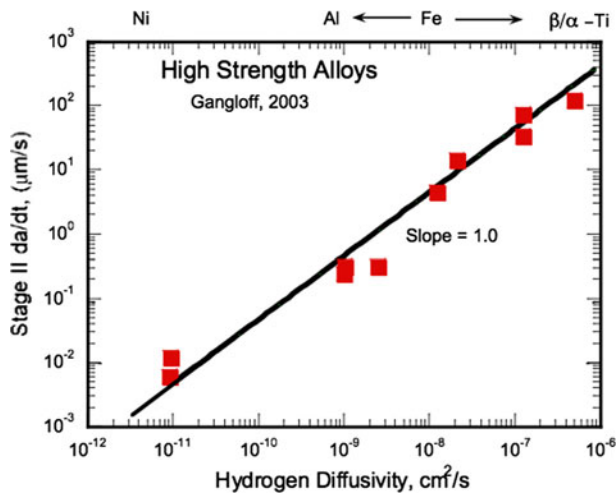


Fig. 16—Parallel shift in threshold for crack growth as a function of pressure in shifting from H2 to D2.



Fig. 15—One-to-one correspondence between hydrogen diffusivity and plateau velocity in several materials.
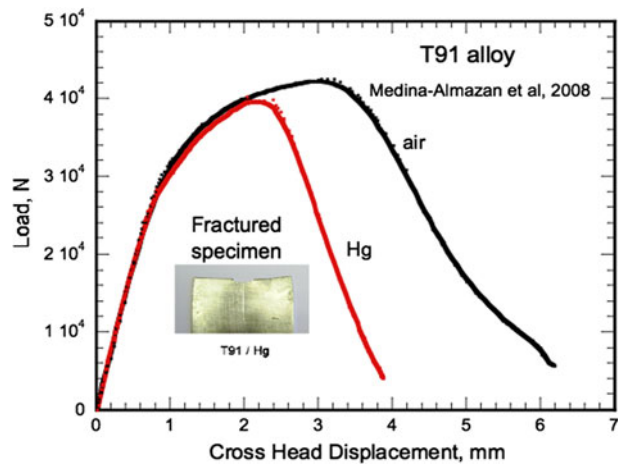


Fig. 17—Load-displacement curves for T91 alloy in air and Hg environments.

The preceding authors considered the fracture problem in the absence of environment. Under aggressive environments, instead of rapid fracture, the crack growth can be subcritical until stage III sets in. Local incremental or subcritical crack growth can be envisioned by the similar mechanisms wherein the ductile-brittle-ductile crack tip growth can occur alternatively to establish a steady-state crack growth. Generally, grain boundary paths are preferred for diffusion, but in their absence (*i.e.*, in single crystals), the subcritical crack growth appears to be crystallographic, in the absence of any trapping mechanism, as in high H concentration alloys. Oriani and Josephic[79] compared the cracking behavior using hydrogen and deuterium in a 4340 alloy, and the results are shown in Figure 16. The threshold variation with gas pressure remains the same for both cases, with the slopes close to 0.5, characteristic of the Sievert's or diffusion mechanism governing the kinetics. The factor of 2 differences in thresholds probably arises due to the difference in the diffusion rates of H *vs* D in the alloy.
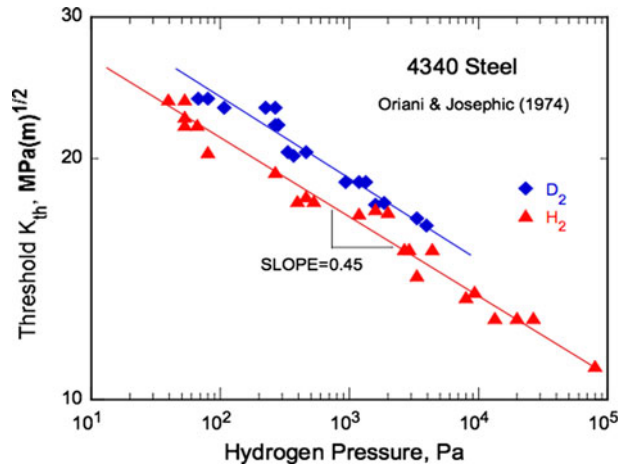
Cracking under LME does not appear to be much different from that in hydrogen. Figure 17 shows that the stress-strain curves are not significantly affected by the liquid metal, except that the fracture strain is considerably less in Hg environment.[80] Such results have been reported earlier.[26–28] Since plastic deformation accompanies the embrittlement as indicated by the significant fracture strain (Figure 17), we have plasticity- or dislocation-induced local cleavage, as evidenced by the "shear-band failure" observed in these materials (Figure 18(a)). Intergranular and cavity nucleation and coalescence modes of crack growth were also noticed (Figures 18(b) and (c)). Hence, based on the fractographic analyses, embrittlement by hydrogen or by liquid metal appears to be somewhat similar, although the kinetics in each could be different.[13,14]

The behavior of SCC crack growth in glass[16] in humid environment is also similar to the LME, as shown in Figure 19. A well-defined threshold may not be there in some glasses, as discussed by Weiderhorn *et al.*,[16] but the mechanics of crack growth remain similar. There is no plasticity associated with the crack
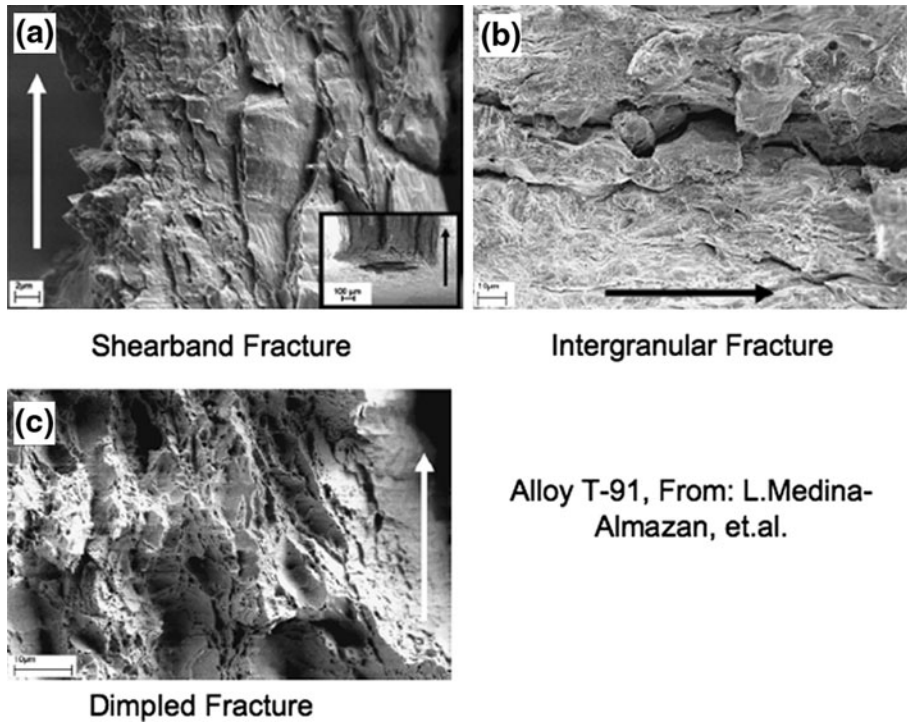
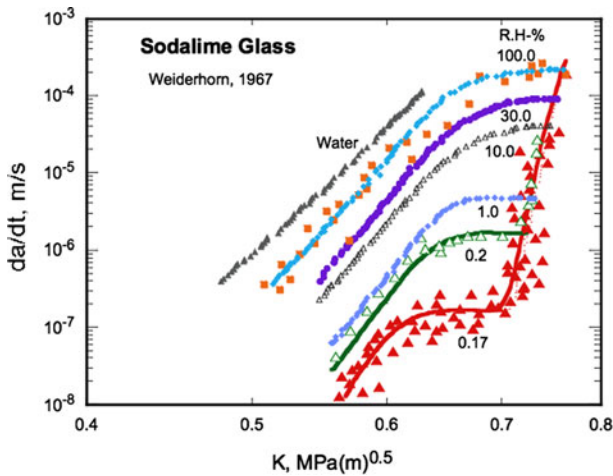Fig. 18—Fracture in Hg environment showing shear band, intergranular, and dimpled fractures in T-91 alloy.



Fig. 19—Crack growth rate *vs* stress intensity in soda-lime glass as a function of relative humidity.



Fig. 20—Crack growth rate as a function of relative humidity at two stress intensity levels for a soda-lime glass.

growth, but the crack tip bonds are stretched enough for the water molecules to attack and reduce their bond strength. Figure 19 shows that the concentration dependence arises as the percentage humidity increases with stage I, and the beginnings of stage II to rapid crack growth characteristics of stage III are observed. Interestingly, in the water environment, no stage II was observed, the behavior similar to that at high H concentrations in metallic systems (Figure 11). The subcritical crack growth occurs essentially maintaining locally Griffith's condition, since there is no plastic dissipation of energy during crack growth. Figure 20 shows crack growth rates at a stress level that

corresponds to stage I and plateau regions as a function of percent humidity. The curves are essentially parallel, indicating that there is no change in the kinetics of the embrittling process. The steady state at any given percent humidity is established by the dynamics of the reaction process at the fast moving crack.

That the diffusion distance is not too far from the crack tip is established by observing the change in the crack growth rate, when the environment is changed. Figure 21 shows the classic work of Hancock and Johnson.[81] Here, they have introduced oxygen intermittently, which blocks the diffusion of H or alters the reaction kinetics at the crack tip. The crack growth rates

Fig. 21—Sudden change in crack growth rates with changing environments at constant remote stress.

decreased rapidly with the introduction of a mixture of hydrogen and oxygen. With the reintroduction of pure H, the recovery of the previous crack growth rates is somewhat slower since it involves elimination of a minute amount of oxygen sticking to the crack tip surfaces. More drastic effects we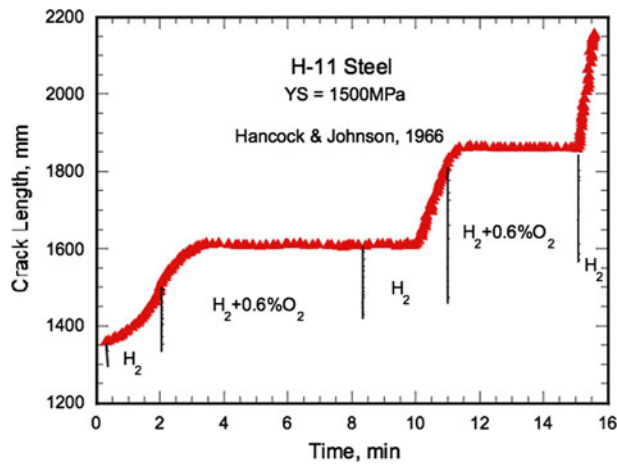re observed with the introduction of oxygen by Vehoff and Rothe[64] in Fe-2.6 pct Si and in Ni. The implication of these results is that the diffusion distances are not too far from the crack tip, since the effects of new environments set in rapidly. Similarly, the change of crack tip stresses by overload or underload can affect the kinetics of crack growth. Incubation times, for example, can be drastically affected by overloads and underloads, and the evaluation of these effects in terms of internal stresses is presented elsewhere.[82]

### C. Crack Growth Kinetics

We have thus far presented several aspects of chemically assisted crack growth results from the literature under various environments affecting the SCC behavior of several alloys. There are several mechanisms proposed in the literature, such as HELP, hydrogen enhanced decohesion (HEDE), internal hydrogen assisted cracking, hydrogen environment assisted cracking, etc., explaining the data. It is evident from these reviews that there is no clear consensus regarding the governing mechanisms. Each model explains a part of the governing mechanisms for a system, but the complexity of the mechanisms prevents any generalizations. In spite of this complexity, there are some common features that seem to govern the behavior in many systems. There is a discrete mechanical threshold below which no crack growth occurs. There is also some kind of saturation effect in terms of chemistry defining a maximum contribution from a given environment in assisting crack nucleation and growth. In ceramic systems such as glasses, there is no evidence of crack tip plasticity and the governing mechanism occurs at the crack tip. Owing to fast crack growth rates in these brittle materials, transportation of the chemical species

to the fast moving crack can become a controlling factor.[16,59,60] A somewhat similar situation arises in some cases in the LME of alloys, where viscous flow of the liquid toward the fast moving crack could be the rate determining step.[83] If this process is faster, the reaction at the crack via chemisorption or stress-induced dissolution or, in some cases, diffusion along grain boundaries ahead of the crack tip or normal lattice diffusion in the case of single crystals will be the rate determining factor. Consensus from experiments and numerical analysis is that for the precracked fracture mechanics sample or notched tensile specimens, peak concentration of the embrittling species occurs at the notch tip, or at the most slightly away from the notch tip in ductile alloys or in larger root radii notches. In all these cases, the microcrack formation is limited to within the plastic zone of the notches. In the case of internal hydrogen, the diffusion from bulk toward the crack tip has to occur, and hence, the kinetics of embrittlement is slower than that in external environment, which is close to the crack tip. Because hydrogen is very mobile, it can get trapped by local stress concentrations. Hence, depending on the H concentration, the fracture mechanisms change from intergranular, to cleavage, to void formation at carbides, thus affecting the kinetics of the crack growth.

In general, environment affects a material in two ways. In metallic systems, it enhances the crack tip slip activity, thus contributing to local ductility. This is accomplished predominantly by lowering the energy needed for dislocation emission at the crack tip. It can also reduce the resistance to dislocation mobility either by the reduction of lattice resistance or by shielding dislocation stress fields from mutual retardation. Hence, crack tip plasticity seems to be accompanying most of the embrittling process, lending to the proposed mechanisms such as HELP.[14,82] The second aspect is that it reduces the cohesive forces that bind the atoms, say, by the reduction of the surface energy. This leads to embrittlement with fracture occurring at much lower stress than that without the environment. Generally, enhanced ductility and the enhanced embrittlement are mutually opposing factors, contributing much of the controversy in the literature in terms of the rate controlling processes. Here, we are not including the crack tip dissolution process, which may occur in some special cases.[49–52]

Any SCC mechanism, therefore, should have two factors. One that is responsible for ductility enhancement and the other that is the embrittlement process by a reduction in the cohesive forces. In this regard, the work of Vehoff and Roth[64] on single crystals of Fe-2.6 pct Si and Ni is noteworthy. They show that crack growth occurs at a constant angle $\alpha$ smaller than $\theta$, where $\alpha$ is the crack-mouth-opening angle and $\theta$ is the slip plane angle (Figure 22). From McClintock's analysis,[84] such a condition is possible only if there are two interdependent processes: (1) crack opening mechanism and (2) crack resharpening mechanism. The crack opening mechanism is due to the slip process, while the crack resharpening mechanism is provided by the decohesion processes involving cleavage or faceted mode of crack growth. This is schematically shown in

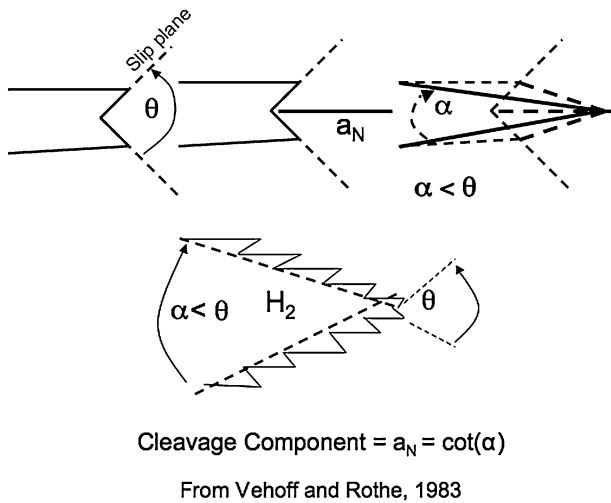Cleavage Component = $a_N$ = cot($\alpha$)

From Vehoff and Rothe, 1983

Fig. 22—Dislocation slip and cleavage crack growth occurring sequentially, resulting in constant crack mouth opening angle, as observed by Vehoff and Rothe.
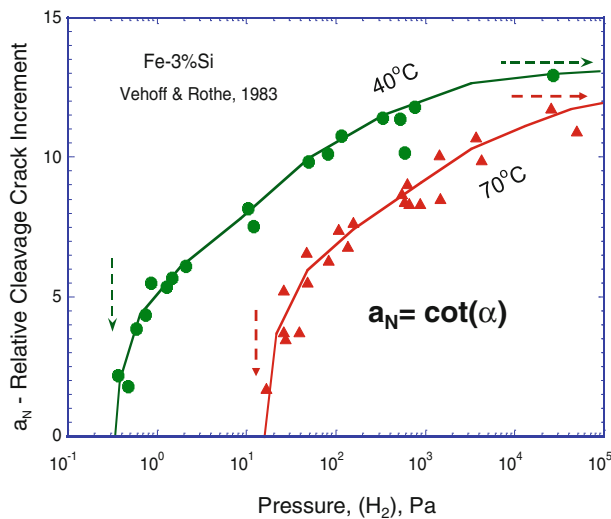


Fig. 23—Change in cleavage component with hydrogen pressure at two different temperatures in Fe-3 pct Si.

Figure 22. The dislocation shear can also occur asymmetrically alternating above and below the crack plane. Considering that the crack increment during the dislocation shear is small, Vehoff and Roth[64] showed that the cleavage component, $a_N$, does not depend on crack growth rate; hence, hydrogen transport processes are not rate limiting. On the other hand, the cleavage component depends on the hydrogen pressure (which relates to H concentration), as shown in Figure 23. With increasing hydrogen pressure, the cleavage component increases at the expense of the shear component, making the crack sharper. We recall that with the increase in hydrogen concentration, the crack growth mechanism in nickel-base alloy (Figures 9(a)) shifts from microvoid formation and coalescence to faceted mode of crack growth, in single crystals. Figure 23 shows that the cleavage contribution reaches an upper limit with high hydrogen concentration, and this limit depends on the

temperature. The upper limit of the cleavage component indicates that plasticity always accompanies at any level, even though its contribution decreases at high H concentrations. At low concentrations that one can measure, the cleavage component is small, while the growth occurs predominately by the plasticity induced process, where the low hydrogen that segregates to inclusions or carbides sites causes void nucleation and growth. The analysis is self-consistent and compatible with fractographic observations (as in Figure 12). One of the consistent findings is that cleavage in bcc materials occurs predominately along the {100} planes and in fcc materials along the {111} slip planes. The alternate mechanisms of slip and cleavage seem to occur at the microscale. With decreasing yield stress, the plastic zone increases and the scale of plasticity is enlarged. The mechanism is somewhat similar to the HELP mechanism in the sense that the plasticity helps in the cleavage process. However, no void formation was found in Ni and Fe2.6 pct Si single crystals by Vehoff and Roth,[64] even though it has been noted in other alloys, particularly when H concentration is low.

### D. Alternating Slip and Cleavage

Dislocation nucleation and cleavage seem to alternate in some form, giving rise to crack tip embrittlement. This appears to be true even in LME where intermittent dislocation nucleation opens up the crack for the flow of the liquid to embrittle the crack tip region.[85] Alternately, the slip may break up the passive film formed there by exposing it to the corrosive environment. Diffusion of the embrittling chemical element ahead of the crack tip appears to be governing in some systems with activation energy close to the diffusion energy. Gerberich and Chen[6] and many authors have emphasized that the plastic deformation helps to buildup hydrostatic stresses ahead of the crack tip to facilitate diffusion, condensation, and microcrack nucleation ahead of the main crack. Thus, plasticity in this case helps in building the hydrostatic stresses facilitating diffusion. Subcritical crack growth is ensured by having this process intermittently occurring with the crack blunting, diffusion, and cleavage and back to crack blunting. Crack tip blunting by dislocation generation is inevitable in most ductile systems, since materials cannot sustain infinite stresses at the crack tip. The implication is that we need to consider not a sharp crack but a microscopically blunted crack for analysis.

The detailed analysis of crack tip blunting and dislocation nucleation at the crack tip as a means of separating the ductile vs brittle behavior has been proposed by Rice and Thomson,[86] and subsequently by Rice and co-workers.[23,86–93] However, we are concerned here not with the mutually exclusive blunting vs cleavage, but one leading to the other, i.e., blunting leading to cleavage. Analysis of crack tip stress fields in elastic-plastic materials has been computed using the Hutchinson–Rice–Rosengren (HRR) analysis, but those stresses pertain to sharp cracks and are valid at distances away from the blunted crack tip. There are no analytical solutions for the stress fields within the region close to a

blunted crack tip, where the corrosion reactions take place. Rice and Johnson[76] used an approximate analysis of the stress fields to evaluate the growth of pre-existing voids ahead of the crack (notch) tip, by combining slip-line fields with HRR fields. Hirose and Mura[61] also used slip line field theory along with dislocation analysis to evaluate the nucleation of the microcracks ahead of the notch, but within the plastic zone of the notch. They have considered the slip plane to be the same as the cleavage plane. Ritchie *et al.*[78] used a similar approach to evaluate the cleavage fracture of carbides located at one or two grains ahead of the main crack. A common factor in all these analyses is the recognition that blunting is inherent and blunting eventually leads to some cleavage, particularly if cleavage conditions are satisfied. Reduction of surface energy to facilitate the cleaving process would then lead to an embrittlement phenomenon.

In the corrosion process, we are combining the mechanics of the growth of a blunted crack with a time-dependent phenomenon involving the diffusion of the embrittling species to a maximum stress concentration to initiate local or incremental fracture. Continuum analysis using blunted crack tip (pre-existing) combined with diffusion kinetics by Taha and Sofronis[94] yielded the following results that are of interest. In tandem with the other analyses, the peak hydrostatic stresses occur within one to two units of $(x/\rho)$, where $x$ is the distance measured from the crack tip along the $X$-axis and $\rho$ is the crack tip radius. The hydrogen concentration gradually reaches a maximum and saturates at the maximum hydrostatic stress level, in agreement with Gerberich analysis.[6] Importantly, since diffusion of H is rapid in steels, it takes a very short time to reach a steady state since distances are very close to the crack tip. Thus, the reaction occurs within the distances of $\rho$ from the blunted crack, where analyses based on sharp crack profiles become less reliable. Note that in the preceding analyses, although blunted crack tips (preexisting) are considered, the change in the blunting configuration due to plasticity or dislocation generation is not considered.

Beltz *et al.*[23] analyzed the problem of the blunting *vs* cleavage for a blunt crack by considering the cohesive forces to open a crack ahead of the blunted crack and shear forces for the generation of dislocations on the slip plane. This is an extension of dislocation *vs* crack extension considered earlier by Rice and Thomson[86] and Rice and co-workers.[86–93] Figure 24 schematically presents the problem in question. When a blunted crack of tip radius $\rho$ is stressed, a microcrack can initiate ahead of the blunted crack along the cleavage plane or a dislocation can be emitted on the slip plane. The cohesive force and shear force profiles for these two cases are also shown in Figure 24(a). The required forces to generate cleavage or dislocation are represented by $G_{clea}$ and $G_{disl}$, respectively, in Figure 24(b). Beltz *et al.* consider several possibilities of interest. From our point of view, the case illustrated in Figure 24(b) is of interest, where the $G_{disl}$ is initially low when $\rho$ is small, favoring dislocation generation, which increases $\rho$. However, with increasing $\rho$, the curves cross over giving rise to cleavage mode. Initially,
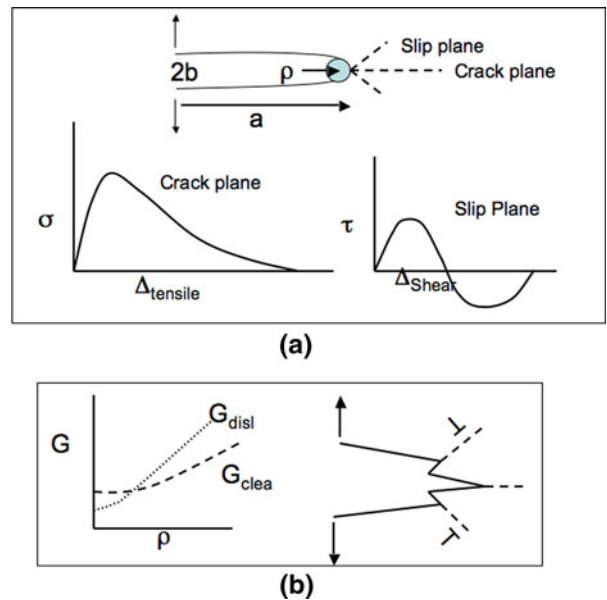


Fig. 24—Illustration of the growth of a blunted crack by slip and cleavage, following Beltz *et al.*
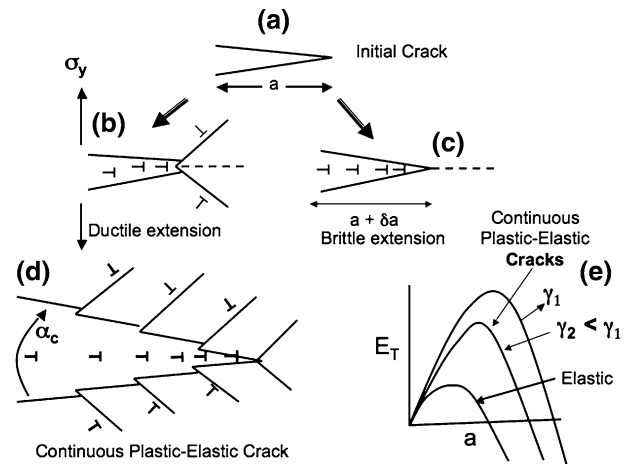


Fig. 25—Discrete dislocation model of crack growth by sequential slip and cleavage crack growth.

blunting is favored but, subsequently, the cleavage takes over resulting in brittle failure. In all the cases that they considered, crack eventually blunts or cleaves depending on the functional values of $G_{clea}$ *vs* $G_{disl}$ in relation to the actual crack tip driving force, $G_c$.

Considering the Vehoff and Roth analysis[64] in Figure 22, we can reformulate the problem, as shown schematically in Figure 25. If we consider a hypothetically sharp fatigue precrack of length $a$ and apply a static load, two possibilities can arise: dislocation generation on the slip planes or brittle crack extension by an increment $\delta a$. Dislocation generation also contributes to small crack length increment. Crack blunts by dislocation generation while it resharpens by cleavage extension. If the dislocations on the slip plane saturate, further generation of them is hindered due to back stresses by all the previously generated dislocations,

while the hydrostatic tensile stress field becomes increasingly significant ahead of the blunted crack tip. The crack will pop open on the cleavage plane making the crack tip sharp, which again can emit dislocations. The processes of blunting and cleavage cycle can continue until the crack becomes unstable. This is what Vehoff and Rothe[64] experimentally found as the growth of crack with a constant crack mouth opening angle, α, the angle decreasing with increasing H pressure. Thus, with decreasing γ, the cleavage component increases in relation to the blunting component. Analytical formulation of this problem is rather difficult. A discrete dislocation analysis of the problem is possible following our earlier work on the growth of a continuous elastic-plastic crack.[94,95] Figure 25 shows schematically the dislocation formulation of the crack and the associated growth. The calculations were done for a given applied stress, lattice friction stress on the slip plane and γ, the surface energy. Starting from a very small crack, the crack is either allowed to emit dislocations on the slip plane or extend in cleavage mode on the cleavage plane depending on whatever process has lower elastic strain energy. The strain energy can be computed by taking into consideration self-energies, interaction energies, and the work done by applied and frictional stresses. After emitting a dislocation, the crack has a choice again to emit more dislocations or to extend as a cleavage crack. Depending on the friction stress (proportional to yield stress) and γ, we found that crack goes through an alternate process of emitting dislocations, thereby getting blunted, and subsequently extending in cleavage mode, thereby resharpening itself. The process occurs continuously in sequence until the total energy of the entire system goes through a maximum with respect to crack length, leading to a Griffith type of instability condition. This is shown schematically in Figure 25. By extending the analysis of Beltz et al.[23] in terms of crack tip driving forces, the interplay of cleavage vs blunting can be schematically represented by Figure 26. This type of shuttling deformation-cleavage process results in a constant α during corrosion crack growth, as stated by Vehoff and Roth.[64] The cleavage crack extension can be thought of as a microcrack formation ahead of the crack tip (but close to the crack tip), which is energetically facilitated by the reduction in surface energy due

to diffusion of the embrittling species. The time-dependent aspect comes in terms of accumulation of the needed hydrogen (for example) to facilitate the crack nucleation due to the stress fields of the blunted macrocrack. Discrete dislocation analysis will provide a convenient means of accounting properly the image forces exerted by the crystal dislocations or microcrack. Such an analysis is being done currently and will be published later. We noted earlier that the faceted growth occurs on the cleavage plane in bcc materials, while it occurs on the slip plane in some fcc materials. The microcrack nucleation can be thought of as occurring either on the cleavage plane or on the slip plane, as shown in Figure 27. The reduction in elastic energy is accounted for by the absorption of all the slip dislocations on that plane, as considered by Gilman.[32] Thus, the mechanisms combine HELP, HEDE, etc., in a generic sense. Void formation can be facilitated by the presence of secondary traps such as carbides or inclusions, but it is not essential, as indicated by the studies of Vehoff and Rothe.[64] If carbides are present ahead of the main crack within the region of the peak stress, then, instead of a microcrack, a microvoid can nucleate heterogeneously leading to microvoid formation and coalescence as a mechanism of crack growth. With increasing yield stress, the process gets shifted closer to the crack tip with the attendant decrease in incubation times and the threshold stress for nucleation. The run-out stress intensity indicates that some blunting and resharpening has to occur for stress corrosion crack growth. Two examples show the transition of fracture from ductile-cleavage-ductile fracture in H-11 high-strength steel[96] under internal hydrogen (Figure 28(a)) and in Al-6Zn-3Mg alloy,[97] showing a transition from ductile–quasi-cleavage/grain boundary–ductile fracture in 3 pct NaCl (Figure 28(b)). These examples of static stress corrosion fracture surfaces support the mechanism described in Figures 26 and 27.

## III. SUMMARY AND CONCLUSIONS

We have examined the published data on subcritical crack growth in chemical environments such as aqueous, external/internal H, presence of internal embrittling species, LME in metals, alloys, and ceramics. From the trends in the data, we can identify some generic
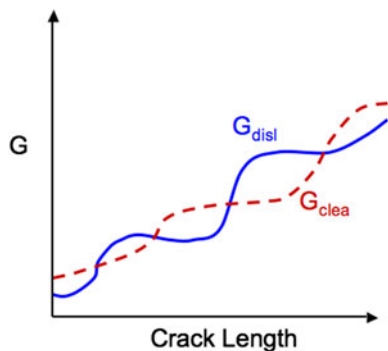


Fig. 26—Schematic illustration of how crack tip force required to cleave and dislocation glide can alternate to give crack growth with constant crack mouth opening angle observed in experiments.
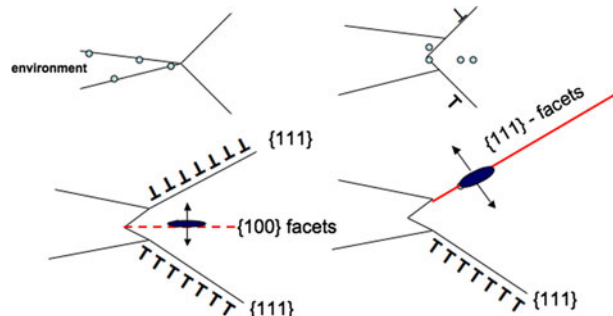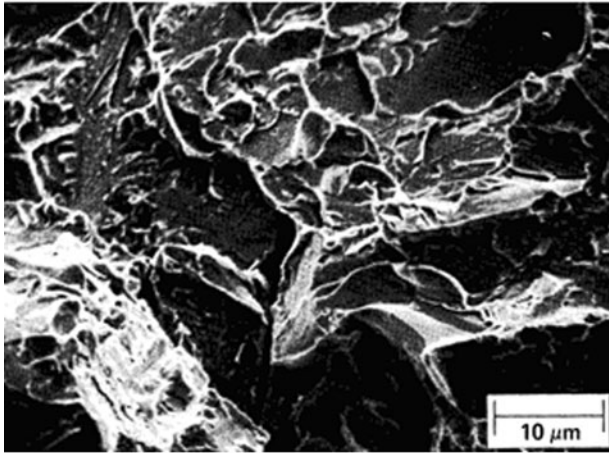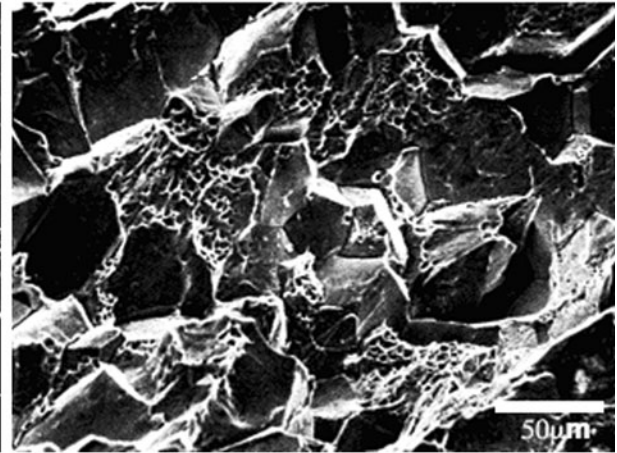


Fig. 27—Dislocation model describing faceted growth along a cleavage plane or a slip plane.

**H-11 Steel, internal Hydrogen (Nelson 1983)**

**Al-6Zn-3Mg, 3% NaCl (Scully 1971)**

(a)

(b)

Fig. 28—Two examples showing the transition of fracture from ductile-cleavage-ductile in (*a*) H-11 high-strength steel under internal hydrogen and in (*b*) Al-6Zn-3Mg alloy showing a transition from ductile–quasi-cleavage/grain boundary–ductile fracture in 3 pct NaCl. These two examples of static stress corrosion fracture surfaces support the mechanism described in Figs. 26 and 27.

principles involved in the time-dependent subcritical crack growth. In general, the crack growth behavior of most materials is somewhat similar, with well-defined thresholds, stage I rapid crack growth, stage II with a plateau in growth rates independent of stress intensity, and finally overload fracture. In many of these cases, there is a measurable incubation time for the crack growth initiation, which depends on the applied stress intensity and concentration and the nature of the embrittling chemical species. The diffusion may be a governing variable, but in some cases, crack tip reactions that provide the embrittling element can be slower by controlling the process. In the liquid metals, the viscous flow or the transport of the reactant products could be controlling, while in solid metal embrittlement, diffusion can be governing. In all cases, there appears to be threshold stress intensity as a function of concentration of the embrittling element, indicating a saturation effect. It affects the crack tip plasticity thereby affecting crack growth kinetics, although there are other considerations that become important and these are being analyzed separately. Crack growth stages depend on the concentration with the plateau region (stage II) present only in the limited concentration range.

Embrittlement and plasticity are not mutually exclusive as intuition leads us to believe. Continuous plastic crack growth can occur by this process, as was analyzed earlier. Corrosive environment can enhance dislocation nucleation and its mobility as well as the cleavage crack nucleation by the reduction of surface energy. The interplay of both crack tip plasticity and cleavage modes can alternate, generating a blunting-cleavage cycle that facilitates corrosion crack growth with associated plasticity. One may call this HELP or HEDE, but it can be simply visualized as an alternating process dictated by changing the crack tip driving force. At low hydrogen concentrations and when carbides or inclusions can act as traps, localized void nucleation, growth, and coalescence with the main crack can contribute to corrosion crack growth in some systems. More detailed analysis of the blunting-cleavage mode of crack growth is needed. A discrete dislocation model is suggested.

## ACKNOWLEDGMENTS

## REFERENCES

1. A.R.C. Westwood, C.M. Preece, and M.H. Kamdar: in *Fracture*, H. Leibowitz, ed., 1971, p. 13.
2. M.H. Kamdar: *Prog. Mater. Sci.*, 1973, vol. 15, pp. 289–374.
3. A.R. Troiano: in *Hydrogen in Metals*, I.M. Bernstein and A.W. Thompson, eds., ASM INTERNATIONAl, Materials Park, OH, 1974, pp. 3–15.
4. M.O. Speidel:, in *Hydrogen in Metals*, I.M. Bernstein and A.W. Thompson, eds., ASM INTERNATIONAL, Materials Park, OH, 1974, pp. 249–76.
5. H.H. Johnson: in *Hydrogen Embrittlement and Stress Corrosion Cracking*, R. Gibala and R.F. Hehemann, eds., ASM, Metals Park, OH, 1984, pp. 3–27.
6. W.W. Gerberich and S. Chen: in *Environment Induced Cracking of Metals*, R.P. Gangloff and H.B. Ives, eds., NACE, Houston, TX, 1990, pp. 167–86.
7. R.A. Oriani: *Berichte Bunsen Gesellschaft Phys. Chem.*, 1972, vol. 76, pp. 848–57.
8. R.A. Oriani: in *Stress Corrosion Cracking and Hydrogen Embrittlement of Iron Base Alloys*, R.W. Stahle, J. Hochman, R. McCright, and J. Slater, eds., NACE-5, National Association of Engineers, Houston, TX, 1971, pp. 32–50.
9. R.P. Wei: in *Hydrogen Effects in Metals*, I.M. Bernstein and A.W. Thompson, eds., TMS, Warrendale, PA, 1981, pp. 677–89.
10. A. Turnbull: *Corrosion*, 2001, vol. 57, pp. 175–89.
11. R.P. Gangloff: in *Comprehensive Structural Integrity*, I. Milne, R.O. Ritchie, and B.Karihaloo, eds., Elsevier, New York, NY, 2003, vol. 6.
12. S.P. Lynch: *Eng. Fail. Anal.*, 1974, vol. 1, pp. 77–90.
13. S.P. Lynch: *Mater. Charact.*, 1992, vol. 28, pp. 279–89.

14. S.P. Lynch: in *Hydrogen Effects in Materials Behavior and Corrosion Interactions Deformations*, N.R. Moody, *et al.*, eds., TMS, Warrendale, PA, 2003, pp. 449–86.
15. C.J. McMahon, Jr: *Eng. Fract. Mech.*, 2001, vol. 68, pp. 773–88.
16. S.M. Wiederhorn, S.W. Freiman, E.R. Fuller, Jr., and C.J. Simmons: *J. Mater. Sci.*, 1982, vol. 17, pp. 3460–78.
17. E. Protopopoff and P. Marcus: in *Corrosion Mechanisms in Theory and Practice*, P. Marcus, ed., Marcel Dekker, Basil, 2002, pp. 53–96.
18. C.F. Old: *J. Nucl. Mater.*, 1980, vol. 92, pp. 2–25.
19. M.M. Hall, Jr.: *Corr. Sci.*, 2009, vol. 51, pp. 225–33.
20. C.D. Beachem: *Metall. Trans.*, 1972, vol. 3, pp. 437–51.
21. B. Lawn: *Fracture of Brittle Solids*, 2nd ed., University Press, Cambridge, United Kingdom, 1995.
22. S.M. Mikheevskiy and G. Glinka: *Int. J. Fatigue*, 2009, vol. 31, pp. 1828–36.
23. G.E. Beltz, D.M. Lipkins, and L.L. Fisher: *Phys. Rev. Lett.*, 1999, vol. 82, pp. 4468–71.
24. N. Bandhopadhyay, J. Kamada, and C.J. McMahon, Jr.: *Metall. Trans. A*, 1983, vol. 14A, pp. 881–88.
25. M. Tvrdy: in *Fracture 1977*, D.M.R.Taplin, ed., University of Waterloo Press, Waterloo, ON, Canada, 1977, vol. 2, pp. 255–59.
26. V.I. Likhtman and E.D. Shchukin: *Sov. Phys.–Uspekhi*, 1958, vol. 1, pp. 91–95.
27. A.R.C. Westwood, C.M. Preece, and M.H. Kamdar: *Am. Soc. Met. Trans. Q.*, 1967, vol. 60, pp. 723–25.
28. N.S. Stoloff, R.G. Davis, and T.L. Johnston: in *Environment Sensitive Mechanical Behavior*, A.R.C. Westwood and N.S. Stoloff, eds., Gordon & Beach, NY, 1966, pp. 613–54.
29. M.H. Kamdar and A.R.C. Westwood: *Acta Metall.*, 1968, vol. 16, p. 1335.
30. A.N. Stroh: *Proc. R. Soc.*, 1954, vol. 223A, p. 404.
31. E. Smith and J.T. Barnby: *Met. Sci. J.*, 1967, vol. 1, pp. 56–64.
32. J.J. Gilman: *Trans. TMS-AIME*, 1958, vol. 212, pp. 783–91.
33. T. Mura: *Micromechanics of Defects in Solids*, Kluwer Acadamic Publishers, Dordrecht, 1991.
34. J.P. Hirth: *Metall. Trans. A*, 1980, vol. 11A, pp. 861–90.
35. P. Gordon: *Metall. Trans. A*, 1978, vol. 9A, pp. 267–73.
36. W. Rostoker, J.M. McCaughey, and H. Markus: *Embrittlement by Liquid Metals*, Reinhold Publishing Co., New York, NY, 1960.
37. R.D. Kane, D. Wu, and S.M. Wilhelm: *ASTM STP-1210*, ASTM, Philadelphia, PA, 1993, pp. 181–92.
38. M. Elboujdaini, R. Ghali, and A. Galibois: in *Environmental Induced Cracking of Metals, NACE-5*, R.P. Gangloff and M.B. Ives, eds., NACE-10, Houston, TX, 1990, pp. 365–70.
39. J.A. Beavers, G.H. Koch, and W.E. Berry: *Corrosion of Metals in Marine Environments*, Metals and Ceramics Information Center, Battelle Columbus Labs., Columbus, OH, 1986.
40. S. Lynch: Monash University, Melbourne, Australia, private communication, 2009.
41. W.Y. Chu, X.M. Liu, J.L. Luo, and L.J. Qiao: *Can. Metall. Q.*, 1999, vol. 38, pp. 127–32.
42. A.P. Druschitz and P. Gordon: in *Embrittlement by Liquid and Solid Metals*, M.H. Kamdar, ed., Metallurgical Society of AIME Publications, Warrendale, PA, 1984, pp. 285–316.
43. P. Gordon and H.H. An: *Metall. Trans. A*, 1982, vol. 13A, pp. 457–72.
44. A.P. Druschitz: Ph.D. Thesis, Illinois Institute of Technology, Chicago, IL, 1982.
45. S.P. Lynch: *Mater. Characterization*, 1992, vol. 28, pp. 279–89.
46. M.H. Kamdar: in *Treatise on Materials Science and Technology*, C.L. Briant and S.K. Benerji, eds., Academic Press, New York, NY, 1983, vol. 25, pp. 361–459.
47. W.P Wei and M. Gao: in *Hydrogen Degradation of Ferrous Alloys*, R.A. Oriani, J.P. Hirth, and M. Smialowski, eds., Noyes Publications, Park Ridge, NJ, 1985, pp. 579–607.
48. D.O. Sprowls, M.B. Shumaker, J.D. Walsh, and J.W. Coursen: "Evaluation of Stress Corrosion Cracking Susceptibilty Using Fracture Mechanics Techniques," Final Report Part I, George C. Marshall Space Flight Center, Huntsville, AL, Contract No. NAS 8-21487, May 31, 1973.
49. W.M. Robertson: *Trans. AIME*, 1966, vol. 236, p. 1478.
50. E. Glickman, V. Igoshev, and A. Braginsky: *Phys. Chem. Mech. Surf.*, 1987, vol. 4, pp. 3167–80.
51. E. Glickman: *Interface Sci.*, 2003, vol. 11, p. 451.
52. E. Glickman: *Diff. Def. Forum*, 2007, vol. 264, pp. 141–49.
53. A.K. Vasudevan and K. Sadananda: *Metall. Mater. Trans. A*, in press.
54. N.J.H. Holroyd, G.M. Scamans, and R. Hermann: in *Embrittlement by the Localized Crack Tip Environment*, R.P. Gangloff, ed., TMS-AIME, Warrendale, PA, 1984, pp. 327–47.
55. K.R. Cooper, L.M. Young, R.P. Gangloff, and R.G. Kelly: *Mater. Sci. Forum*, 2000, vols. 331–337, pp. 1625–34.
56. R.E. Ricker: *Mater. Sci. Eng. A*, 1995, vol. A198 (1–2), pp. 231–38.
57. M.M. Hall, Jr.: in *Environment-Induced Cracking of Materials*, S. Shipilov, *et al.*, eds., Elsevier, New York, NY, 2008, pp. 59–68.
58. M.M. Hall and D.M. Symons: in *Int. Conf. on Hydrogen Effects on Material Behavior and Corrosion Deformation Interactions*, R. Jones, *et al.*, eds., TMS, Warrendale, PA, 2002, pp. 811–22.
59. B.R. Lawn: *Mater. Sci. Eng.*, 1974, vol. 13, pp. 277–83.
60. S.W. Freiman, S.M. Wiederhorn, and J.J. Mecholsky, Jr.: *J. Am. Ceram. Soc.*, 2009, vol. 92, pp. 1371–82.
61. Y. Hirose and T. Mura: *Eng. Fract. Mech.*, 1984, vol. 19, pp. 317–29.
62. W.G. Clark, Jr.: *Flow and Fracture*, ASTM STP 631, ASTM, Philadelphia, PA, 1977, pp. 121–38.
63. R.A. Page and W.W. Gerberich: *Metall. Trans. A*, 1982, vol. 13A, pp. 305–11.
64. H. Vehoff and W. Rothe: *Acta Metall.*, 1983, vol. 31, pp. 1781–93.
65. K. Sadananda and P. Shahinian: *Metall. Trans.*, 1981, vol. 12, p. 343.
66. W.W. Gerberich, P. Marsh, S. Hoehn, S. Venkataraman, and H. Huang: *Int. Conf. on Corrosion-Deformation Interactions CDI '92*, Fontainebleau, Les Edition de physique, zone Industrielle de Courtabaeuf, Paris, France, Oct. 1992, pp. 325–53.
67. R.J. Walter and W.T. Chandler: in *Environmental Degradation of Engineering Materials*, M.R. Louthan and R.P. McNitt, eds., VPI Press, Blacksburg, VA, 1977, pp. 513–22.
68. N.R. Moody, R.E. Stoltz, and M.W. Perra: *Res. Mechanica*, 1986, vol. 18, p. 1.
69. N.R. Moody, M.W. Perra, and S.L. Robinson: *Scripta Metall.*, 1988, vol. 22, p. 1261.
70. J.A. Lillard R.G. Kelly, and R.P. Gangloff: *Corrosion '97*, NACE, Houston, TX, 1997, paper no. 197.
71. K. Endo, K. Komai, and I. Yamamoto: *Bull. MSME*, 1981, vol. 24, pp. 1326–32.
72. P.D. Hicks and C.J. Altestter: *Metall. Trans. A*, 1992, vol. 23A, pp. 237–49.
73. B. Cox: *J. Nucl. Mater.*, 1990, vol. 170, pp. 1–23.
74. M.O. Speidel: *Metall. Trans. A*, 1975, vol. 6A, pp. 631–51.
75. W.G. Clarke, Jr.: *J. Mater. Energy Sys.*, 1979, vol. 1, pp. 33–40.
76. P.S. Pao and R.P. Wei: *Scripta Metall.*, 1977, vol. 11, p. 515.
77. J.R. Rice and M.A. Johnson: in *Inelastic Behavior of Solids*, M.F. Kanninen, W.F. Adler, A.R. Rosenfield, and R.I. Jaffee, eds., McGraw-Hill Book Company, New York, 1970, p. 641.
78. R.O. Ritchie, J.F. Knott, and J.R. Rice: *J. Mech. Phys. Solids*, 1973, vol. 21, pp. 395–410.
79. R.A. Oriani and P.H. Josephic: *Acta Metall.*, 1977, vol. 25, pp. 979–88.
80. L. Medina-Almazan, T. Auger, and D. Grose: *J. Nucl. Mater.*, 2008, vol. 376, pp. 312–16.
81. G.G. Hancock and H.H. Johnson: *Trans. TMS-AIME*, 1966, vol. 236, pp. 513–16.
82. A.K. Vasudevan and K. Sadananda: *Metall. Mater. Trans. A*, DOI:10.1007/s11661-010-0470-5.
83. H.S. Nam and D.J. Srolovitz: *Acta Mater.*, 2009, vol. 57, pp. 1546–53.
84. C.D. Beachem: *Metall. Trans.*, 1972, vol. 3, pp. 437–51.
85. F.A. McLintock: *J. Fract. Mech.*, 1968, vol. 4, p. 101.
86. J.R. Rice and R. Thomson: *Phil Mag.*, 1974, vol. 15, p. 567.
87. J.R. Rice and J.S Wang: *Mater. Sci. Eng.*, 1989, vol. A107, pp. 23–40.
88. G.E. Beltz and J.R. Rice: in *Modeling the Deformation of Crystalline Solids*, T.C. Lowe, A.D. Rollett, P.S. Follansbee, and G.S. Daehneds, eds., The Minerals, Metals and Materials Society (TMS), Warrendale, PA, 1991, pp. 457–80.
89. J.R. Rice and G.E. Beltz: *J. Mech. Phys. Solids*, 1994, vol. 42, pp. 343–60.
90. G.E. Beltz and L.B. Freund: *Phys. Status Solidi (b)*, 1993, vol. 180, p. 303.

91. D.M. Lepkin, G.E. Beltz, and L.L. Fisher: *Mater. Res. Soc. Proc.*, 1999, vol. 539, pp. 49–56.
92. G.E. Bletz and J.R. Rice: *Acta Metall. Mater.*, 1992, vol. 40, pp. s321–s331.
93. D.M. Lepkin and G.E. Bletz: *Acta Mater.*, 1996, vol. 44, pp. 1287–91.
94. A. Taha and P. Sofronis: *Eng. Fract. Mech.*, 2001, vol. 68, pp. 803–37.
95. K. Sadananda, K. Jagannadham, and M.J. Marcinkowski: *Phys. Status Solidi (a)*, 1977, vol. A44, pp. 633–733.
96. H.G. Nelson: in *Embrittlement of Engineering Alloys*, C.L. Briant and S.K. Banerji, eds.; *Treatise Mater. Sci. Technol.,* Academic Press, New York, NY, 1983, vol. 25, pp. 275–359.
97. J.C. Scully: in *The Theory of Stress Corrosion of Alloys*, J.C. Scully, ed., NATO Scientific Affairs Division, Brussels, 1971, pp. 127–66.